Formation of a copper contact grid on the surface of silicon heterojunction solar cells

© *S.N. Abolmasov* [1], *A.S. Abramov* [1,2], *V.N. Verbitskii* [1,2], *G.G. Shelopin* [1], *A.V. Kochergin* [1,3], *E.I. Terukov* [1,2,3]

[1] R&D Center of Thin Film Technologies in Energetics under the Ioffe Institute LLC,
194064 St. Petersburg, Russia
[2] Ioffe Institute,
194021 St. Petersburg, Russia
[3] St. Petersburg State Electrotechnical University „LETI"
197376 St. Petersburg, Russia
E-mail: tem47@mail.ru

A comparative analysis of various methods of forming a copper (Cu) contact grid on the surface of silicon heterojunction solar cells (SHJ SC) as an alternative to the standard screen printing method using expensive silver-containing (Ag) pastes is presented. It has been shown that the use of inkjet printing for the formation of protective dielectric masks based on an organic polymer and thin buffer metal layers for the growth of a Cu contact grid by electroplating makes it possible to form a contact grid of the required shape and having sufficient adhesion to the surface of SHJ SC. Using this method, double-sided SHJ SC (size $157 \times 157\,\mathrm{mm}^2$) with Cu contact mesh were fabricated, demonstrating an efficiency of 22.9% and an adhesion level of $3-5\,\mathrm{N/mm}$ compared to 22.6% and $1.5-2\,\mathrm{N/mm}$ using a similar contact mesh based on Ag paste.

Keywords: solar energy, monocrystalline silicon, heterojunction solar cell, copper contact grid, electroplating, screen and inkjet printing.

1. Introduction

Today, ground-based solar energetics is 95% based on photovoltaic converters (PVCs) based on single-crystal silicon (c-Si) of p-type (the so-called PERC cells of p-type), which in mass production have practically reached the limit in efficiency at the level of $22-23\%$ [1]. Therefore, the general trend of further development is the transition to more efficient technologies based on the c-Si of n-type, such as PERT, TOPCon and SHJ [2]. Among them, the heterostructure (SHJ) technology has, along with other advantages (low-temperature technological process with the least number of technological operations, maximum two-sidedness factor, etc.), the potential to achieve maximum efficiency values $> 26\%$ [3].

It should be noted that in SHJ technology, as in other c-Si photovoltaic technologies, contact grids are used to collect charge carriers, applied to the surface of the PVCs by screen printing with silver-containing (Ag) paste, which subsequently heat-treated. The distinctive feature of SHJ technology is the use of low-temperature Ag-pastes with the curing temperature of $\sim 200°C$, which is significantly lower than the melting point Ag. Therefore, the conductivity of such low-temperature Ag-pastes is lower and is carried out due to the contact of individual micro- and nanoparticles of Ag, which are the basis of the conductive paste, fixed in the cured polymer matrix. Due to the specifics of the technological process and the high content of Ag, the cost of low-temperature Ag-pastes is higher compared to standard high-temperature Ag-pastes used in PERC PVCs.

At present, the self-cost contribution of silver-containing paste to the material self-cost of c-Si solar panels is $\sim 10\%$ and tends to increase due to the rise in price of silver in recent years. Additionally, as the results of recent studies show, a further increase in the production of c-Si PVCs to the terawatt (TW) level in the future may lead to the shortage of silver and the sharp increase in its cost, which will jeopardize the further development of ground-based solar energetics. The most suitable alternative to silver is copper (Cu). This metal is widely used in microelectronics and electrical engineering as the main material for making conductors, it is almost 2 orders of magnitude cheaper than Ag, and its reserves are more than sufficient for TW-production of c-Si PVCs [4].

To date, there are three main technologies that can significantly reduce or completely eliminate the use of Ag in SHJ PVCs by replacing it with Cu, such as Silver Coated Copper Paste (SCCP $\sim 30\%$ Cu), Smart Wire Connection Technology (SWCT $\sim 50\%$ Cu) and Copper Plating (CP $\sim 100\%$ Cu) [5]. Since SCCP and SWCT technologies still include the standard screen printing method for the formation of the contact grid, this only partially reduces the amount of Ag in SHJ PVCs. While copper electroplating — the CP-method, which this article focuses on, allows complete replacement of Ag by Cu, and also has additional advantages over the screen printing method, as will be seen below.
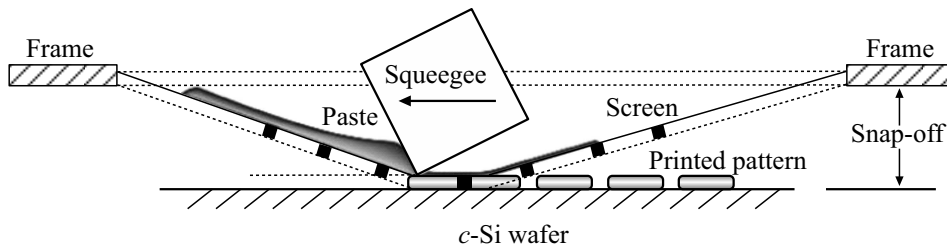
Figure 1. Schematic representation of the process of applying the contact grid on *c*-Si PVCs using the screen printing method.
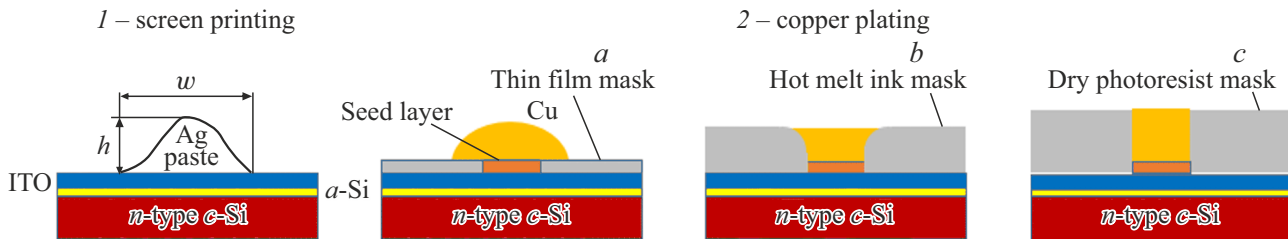
Figure 2. Schematic representation of the contact grid's cross section in the case of using (*1*) screen printing and (*2*) electroplating using various resistant masks.

2. Features of electroplating of Cu-contact grid on surface of SHJ PVCs

Since the electroplating of copper uses electrolytes that have an acidomedium, and the outer surface of the SHJ PVC is covered with transparent conductive layers of indium-tin oxides (ITO), then to protect them from acid exposure and form the contact grid topology formation on their surface etch-resistant dielectric masks are used. On the other hand, the conductivity of the ITO layers is insufficient for uniform current spreading over the entire surface of full-sized SHJ PVCs, which in turn leads to the need to use additional metal layers covering the ITO. These layers can also improve the adhesion of the copper contact grid to ITO. As a rule, metal layers are applied on the ITO surface by magnetron sputtering (PVD), which is widely used to form ITO layers in the mass production of SHJ PVCs. To create etch-resistant dielectric masks, various methods can be used up to photolithography [6], borrowed from microelectronics, where it, along with electrochemistry, has been successfully used to create copper contacts over the past few decades. However, it should be noted that the productivity of modern photolithography systems is ~ 100 wafers/h, while the productivity of modern screen printers for *c*-Si PVCs exceeds 3000 wafers/h, and for PVD systems can reach 10 000 plates/h [7]. Therefore, in the following, we will consider methods for creating etch-resistant dielectric masks and seed metal layers that are compatible with the mass production of SHJ PVCs, using screen printing as a reference.
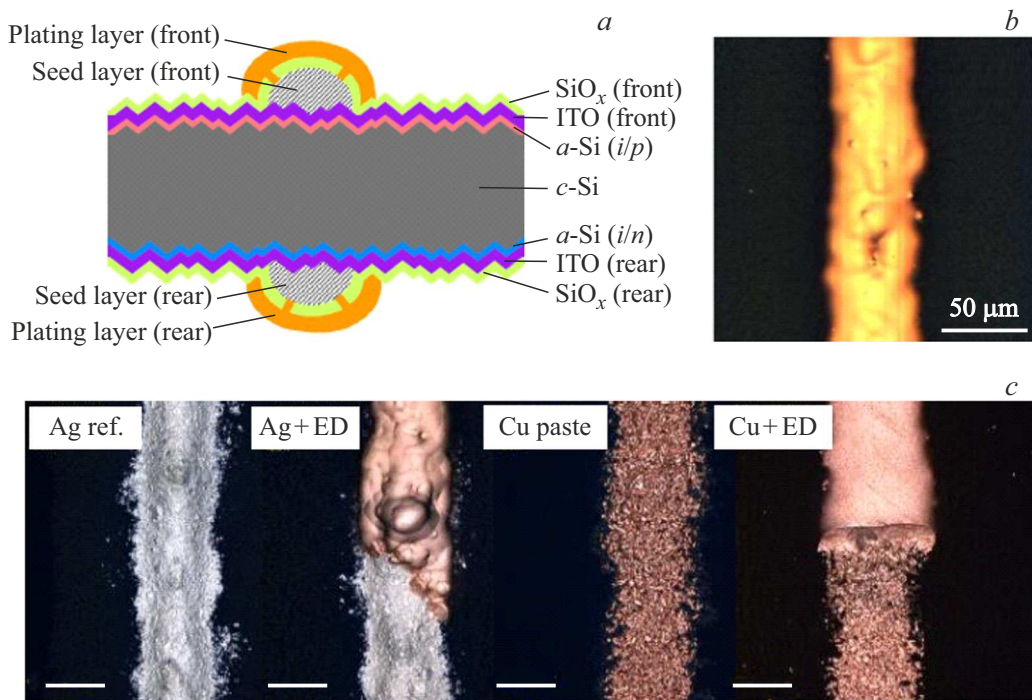
2.1. Screen printing

Screen printing is a standard method for manufacturing contact grids for *c*-Si PVCs, including SHJ PVCs. In this case, the low-temperature Ag-paste is pressed through the holes on the stencil surface, which define the geometry of the contact grid, as seen in Fig. 1.

As a rule, when using screen printing, the contact paths are bell-shaped (see Fig. 2.*1*). However, it should be noted that from the point of view of minimizing optical and electrical losses, the most optimal shape is the contact cross section shown in Fig. 2.*2, c*. At present, the height and width of the contact paths in the mass production of SHJ PVCs using screen printing are at the level of $15-20$ and $40-45\,\mu$m, respectively, i.e., they have the aspect ratio of AR $= h/w \le 0.5$, which could in principle be increased to 1 by using the double printing method. However, this leads to an increased consumption of Ag-paste, i.e., to an increase in the self-cost of SHJ PVCs.

To reduce the consumption of Ag, this method can be used to create a seed layer that forms the geometry of the contact grid, and further growth of copper on its surface through the thin dielectric mask, as shown in Fig. 3. In this case, the thin film of oxide (SiO_x) or nitride (SiN_x) of silicon, deposited using the method of plasma enhanced chemical vapor deposition (PECVD) [9], or ultrathin SAM (self-assembled monolayer) and Al_2O_3 films [10,11].

However, the presence of a thin etch-resistant mask on the ITO surface leads to the lateral growth of the copper contact during electroplating along the surface of the etch-resistant mask, as shown schematically in Fig. 2.*2, a*. This, in turn, leads to loss of adhesion of the contact grid to ITO, as well as to the broadening of the initial Ag-contact grid applied by screen printing. In this case, the size of the broadening

Figure 3. *a* — using screen printing to form a seed layer, which initially sets the geometry of the contact grid for electroplating. *b* — Kaneka process [9]. *c* — CSEM process using Ag- and Cu-pastes and SAM etch-resistant mask [10].

Table 1. Progress in the development of SHJ PVCs with a copper contact grid deposited by electroplating

| Organization	Method	Mask	Width of fingers, μm	Adhesion, N/mm	Area of PVC, cm^2	Max efficiency, %
Kaneka [9]	Screen-printing	PECVD SiO$_x$	45−55	/	239 (M2)	20.8*
SunDrive [13]	Laser exposure	Dry/wet photoresist	15	/	274 (M6)	25.54
Silevo [14]	Laser exposure	Dry photoresist	32	/	239 (M2)	23.1
EPFL/CSEM [10]	Laser ablation	ALD Al$_2$O$_3$/PECVD a-Si	25−40	/	235 (M2)	19.18
CSEM [11]	Screen-printing	ALD Al$_2$O$_3$	40−50	/	222 (M2)	21.0
CSEM [19]	Inkjet printing	Hot melt ink	25−30	4	222 (M2)	24.73
Fraunhofer ISE [17]	NaOH Inkjet etch	PVD Al/AlO$_x$	25−30	0.5−2.3	222 (M2)	22.1
Fraunhofer ISE [12]	Laser ablation	PVD Al/AlO$_x$	25	/	244 (M2)	21.4

Note. * Efficiency of SHJ module is indicated, not PVC.

is approximately equal to twice the height of the copper contact, i.e., with an initial size of 25μm, the width of the contact paths after the completion of the electroplating process will be $\sim 50 \mu$m (see Table 1, Kaneka). It should also be emphasized that in most studies on the formation of a copper contact grid on the surface of SHJ PVC, there are no data on its adhesion to the surface of ITO layers, as can be seen from Table 1.

2.2. Laser exposure

Another method that allows you to quickly form a pattern of the contact grid on the dielectric mask is laser exposure. In this case, the laser can be used directly to remove the material of a thin etch-resistant dielectric mask, as shown in Fig. 4. The advantage of this method is the possibility

of creating narrow contact paths ($15−25 \mu$m, see Table 1) due to the small diameter of the laser beam. However, this method has all the same disadvantages of using a thin mask in the electrochemical process described above. Moreover, laser action on the SHJ PVC surface during the process of removing the material of the etch-resistant mask (laser ablation) can lead to the appearance of additional surface defects, i.e., to a decrease in the efficiency of the SHJ PVC. As can be seen from Table 1, in this case the efficiency does not exceed 21.4%, even in the case of using femtosecond UV lasers [9], which have the least destructive effect.

As practice shows, the use of the thick film photoresist in combination with laser exposure allows to achieve significantly higher efficiency of SHJ PVC when using electroplating of contacts (Table 1, SunDrive [13], Silevo [14]). This is due to the fact that in this case, the laser beam
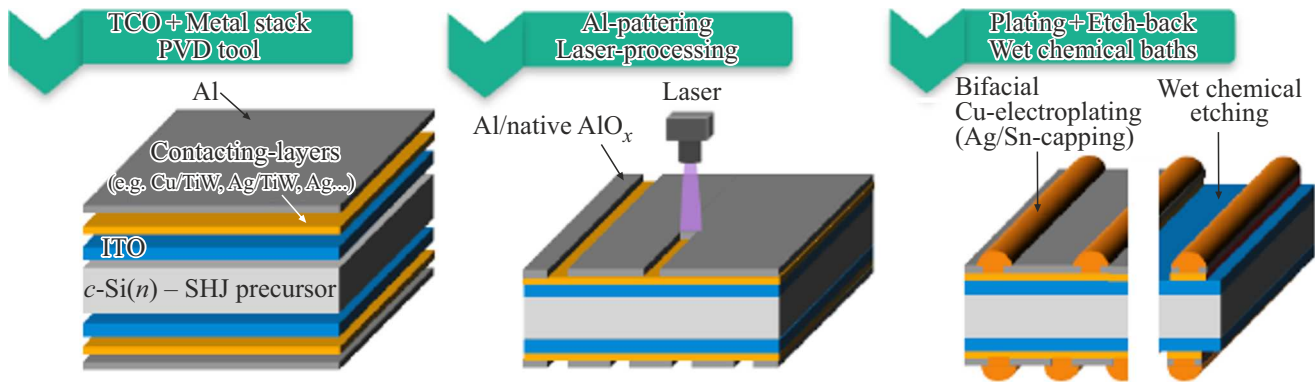
Figure 4. Schematic representation of the NOBLE process using laser exposure (ablation) to form the contact grid pattern developed in Fraunhofer ISE [12].

Table 2. Comparison of specific resistance of various materials for forming contact paths in c-Si PVC

Material	Specific resistance, μOhm · cm
Pure silver (Ag)	1.6
High-temperature Ag-paste (PERC PVC)	$2-3$
Low-temperature Ag-paste (PERC PVC)	$4-5$
Pure copper (Cu)	1.7
Electroplated copper	$1.8-2.6$
100 nm PVD Cu-layer	$3-3.5$

is almost completely absorbed inside the photosensitive material of the film photoresist, for its local polymerization (the so-called exposure stage) with subsequent removal to containers with the developer (development stage). Thus, in this case, the laser does not lead to the formation of additional surface defects and a efficiency decrease of the SHJ PVC. The film photoresist is negative and consists of 3 layers [15]: top polyethylene (PET) layer, inner photosensitive layer and bottom protective polyester (PE) layer. The thickness of the film photoresist can vary from 10 to 100 μm. Unlike standard liquid photoresists, which are applied to the surface of samples by centrifugation, film photoresist is applied using a laminator at a temperature of $100-150°$C, which makes this method acceptable for use on the surface of textured SHJ PVCs. In this case, the PET layer must be removed before the lamination process. Thick film photoresist in combination with laser exposure makes it possible to achieve a completely vertical relief and a minimum width of copper contact paths with AR $= h/w > 1$, as shown schematically in Fig. 2.2, c, and that can lead to an increase in the efficiency of SHJ PVC due to an increase in short circuit current (I_{sc}) and filling factor (FF). The latter depends on the resistance of the contact grid, which is directly proportional to its specific resistance. As can be seen from Table 2, the specific

resistance of galvanic copper is approximately 2 times lower than the resistance of low-temperature Ag-pastes used in SHJ PVCs during screen printing.

Nevertheless, it should be noted that the process of forming a etch-resistant mask in this case is quite complex and includes several stages:

1) pre-treatment of the surface of the film photoresist, including the removal of the PET layer;

2) lamination (may be problematic at thickness of SHJ PVC $< 150 \mu$m);

3) laser exposure;

4) development;

5) drying.

On the other hand, the cost of a film photoresist today is a certain amount of \$/m^2, which makes this technology rather expensive.

2.3. Inkjet printing

Inkjet printing is the simplest method for forming a etch-resistant dielectric mask on the surface of a SHJ PVC. In this case, to achieve the required processing speed, piezoelectric printheads with an operating frequency of ≤ 10 kHz [16] are usually used. Inkjet printing can be used both in the mode of removing the material of the dielectric mask (similar to laser ablation, Fig. 4), and in the mode of applying it. The advantage of the first method is the minimal use of ink, since they are used directly to create a contact grid pattern, i.e., in this case the mask is positive (Fig. 5). However, it should be emphasized that the use of the thin etch-resistant mask leads to the same problems as in the case of screen printing/laser ablation — the growth of galvanic copper above the surface of the protective film, i.e., the broadening of the contact paths and loss of adhesion (Fig. 2.2, a).

On the other hand, when forming a dielectric mask consisting of the ink material (Fig. 6), it is necessary to cover with sketch the surface outside the contact grid (negative mask), i.e., almost the entire surface of the SHJ PVC, which, along with its micron texture, leads to the large consumption of ink, since the thickness of the
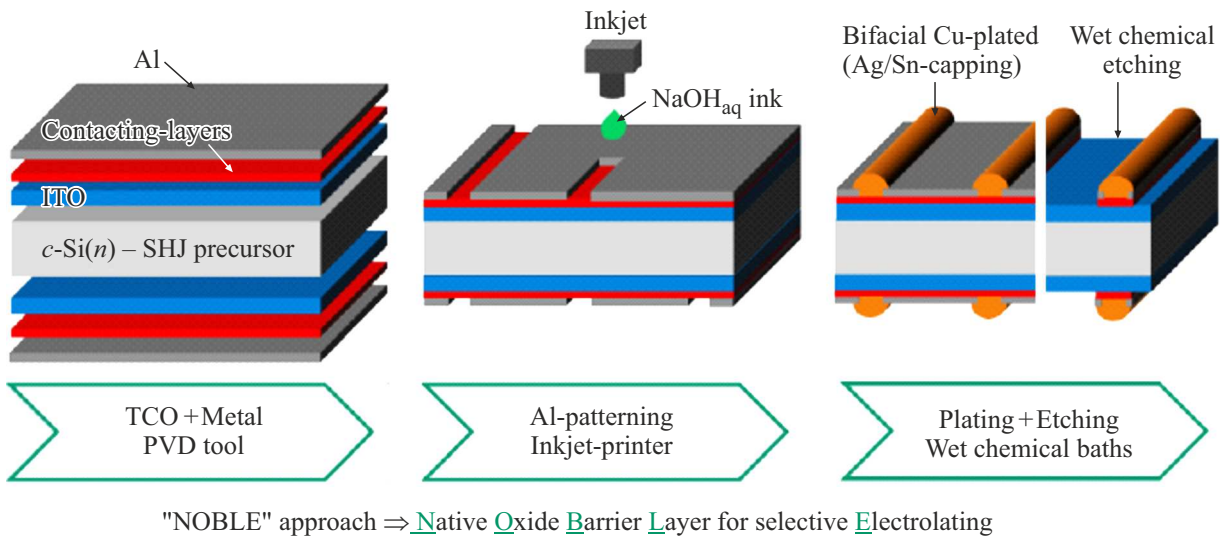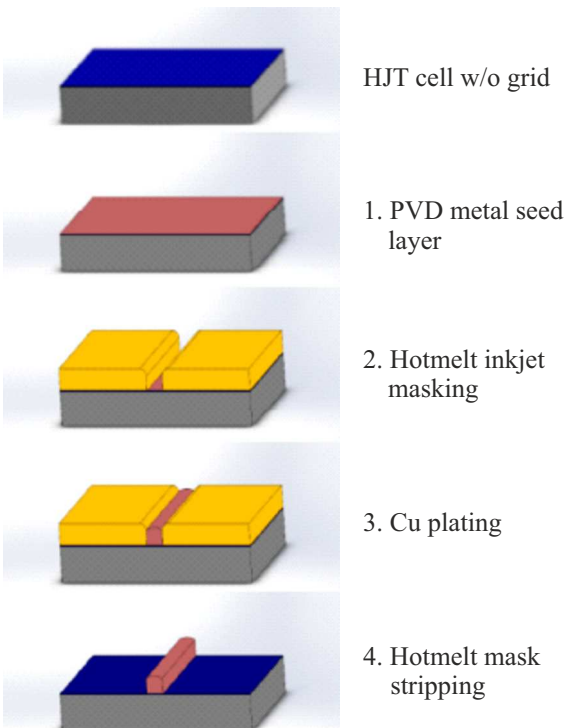
Figure 5. Schematic representation of the NOBLE process developed at Fraunhofer ISE using alkaline etching to form a contact grid pattern using an inkjet printer [17].

mask must be greater than the height of the pyramids on the surface of the SHJ PVC ($\leq 5\,\mu$m). It should also be noted that the mask must be removed after completion of the electroplating process (step *4* in Fig. 6). Therefore, the profitability of this method is determined both by the cost of the ink itself and by the method of its disposal.

Figure 6. Schematic representation of electroplating process developed by CSEM [15,16] in which the geometry of the contact grid is specified by inkjet printing of the organic polymer etch-resistant mask.

According to the estimates of the CSEM research group, the solution to this problem can be the use of fairly cheap ink based on organic polymer — hot-melt ink (hot melt ink (HMI)) [18,19].

Distinctive feature of HMI masks is the round shape of the groove walls that form the copper contact paths during the electroplating process, as seen in Fig. 2.*2*, *b*. Therefore, copper contact paths as they grow can start to expand, taking the form of the HMI mask's walls, which will lead to increased shading and falling I_{sc}. Obviously, the radius of curvature in this case is determined by the size of the HMI drop and its interaction with the sample surface, which depend on such parameters as ink viscosity, printhead nozzle diameter, ink and sample temperature, printing speed, etc. [16]. The purpose of this work is to select the optimal parameters for inkjet printing using HMI to form copper contact paths with the width of $\leq 40\,\mu$m and to determine their optimal height in order to minimize HMI consumption, as well as to optimize their adhesive properties.

3. Experimental methods

For the fabrication of SHJ PVC, *c*-Si wafers with *n*-conductivity type, 157.35×157.35 mm, with crystallographic orientation $\langle 100 \rangle$, grown by the Czochralski (CZ) method. The specific resistance and thickness of the wafers were $1-3$ Ohm · cm and $150\,\mu$m, respectively. Previously, the wafers went through the stages of chemical texturing and surface cleaning. To deposit intrinsic and alloyed layers of hydrogenated amorphous silicon (*a*-Si:H), industrial reactors VHF−PECVD were used (reactor area 130×110 cm^2, frequency 40.68 MHz) [20]. ITO and metal layers were deposited on both sides of the SHJ PVC using the Oxford PlasmalabSystem400 PVD system. Various combinations
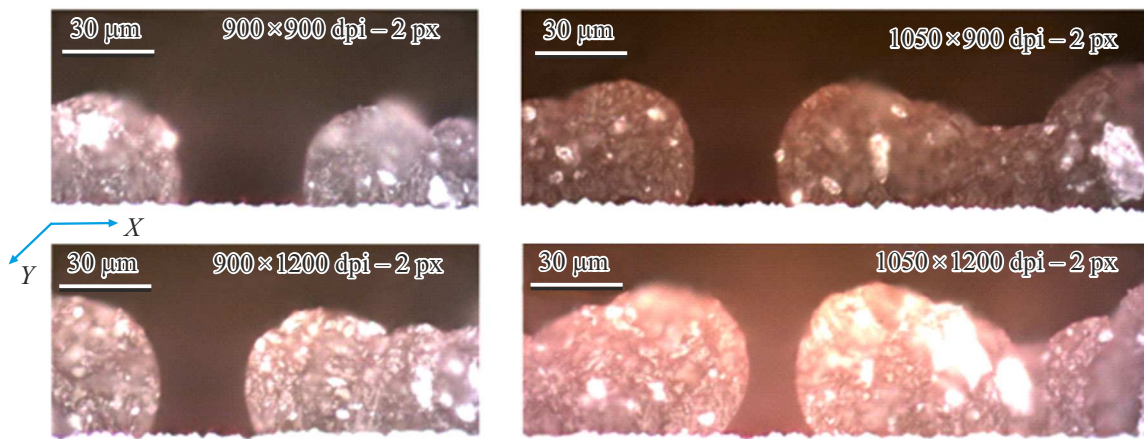
Figure 7. Photo of the cross section for the upper side of the SHJ PVC after the process of applying the etch-resistant HMI mask with an inkjet printer, depending on the printing definition. The area near one of the grooves for the galvanic contact path is shown.

of thin Ti, Cr, NiV, and Cu PVD layers were tested as metal layers to achieve the required adhesion to ITO and lateral conductivity. To form etch-resistant dielectric HMI masks, a PiXDRO LP50 inkjet printer (SUSS Microtec) was used. Wax-based HMIs were used in these experiments. The stage of electroplating of the copper contact grid consisted of the following steps: 1) preliminary surface preparation in acid solutions to remove contaminants and oxides, 2) electroplating of copper contacts in sulfuric acid electrolyte, 3) electroplating of tin using acid electrolytes. The thickness of the formed Sn-coating was $\sim 1.5\,\mu$m, which protected the copper contacts from oxidation. Removal of dielectric HMI masks from the surface of SHJ PVC was carried out in slightly alkaline solutions and solvent solutions, followed by etching of metal PVD layers in acid solutions.

For comparison, the group of SHJ PVCs was also fabricated with the standard grid based on low-temperature Ag-paste applied by screen printing using a printer (ASYS/EKRA E2) and having a height and width of contact paths of about 15 and $40-45\,\mu$m, respectively.

Measurements of current-voltage characteristics (CVC) obtained by SHJ PVC were carried out using the pulsed solar simulator Pasan SpotLight HighCap (1.5 AM, 25°C, 1 Sun). To analyze the relief of the HMI masks and measure the height of the Cu-contact paths, a Nikon Eclipse LV100 optical microscope and an AlphaStep D-120 stylus profilometer were used. The adhesion quality of copper contact paths was measured using a G-5 gram gauge.

4. Results and discussion

Figure 7 shows the effect of increasing the resolution (dpi) of an inkjet printer in the X and Y directions, i.e., across and along the contact paths, respectively, on the shape of the grooves for growing copper galvanic contacts. It can be seen that an increase in dpi in any of the directions

leads to narrowing of groove in the etch-resistant mask, i.e., to the narrowing of the Cu-contact paths, and their geometry acquires a double-concave shape. At the same time, the height of the etch-resistant mask increases due to more ink, and the printing speed drops. From the point of view of minimizing optical and electrical losses in SHJ PVC, it is necessary to strive for the shape of the groove shown in the upper left corner in Fig. 7.

To study the effect of the height of the Cu-contact paths (in the English literature, fingers) on the parameters of the SHJ PVC, the geometry of the contact grid with 4 current-collecting busbars (4BB) was used. With this, the geometry of the grooves in the etch-resistant HMI mask, presented in Fig. 8, was used. In this case, the width of the
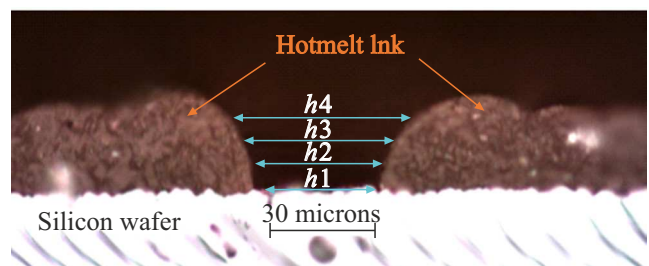
Height	Distance from c-Si surface, μm	Mask opening width, μm
h1	0	35.9
h2	10	38.3
h3	16	44.4
h4	21	51.1

Figure 8. Photo of the cross section for the upper side of the SHJ PVC after the process of applying the etch-resistant HMI mask with an inkjet printer. The area near one of the grooves for the galvanic contact path and its width (average value) depending on the height are shown.
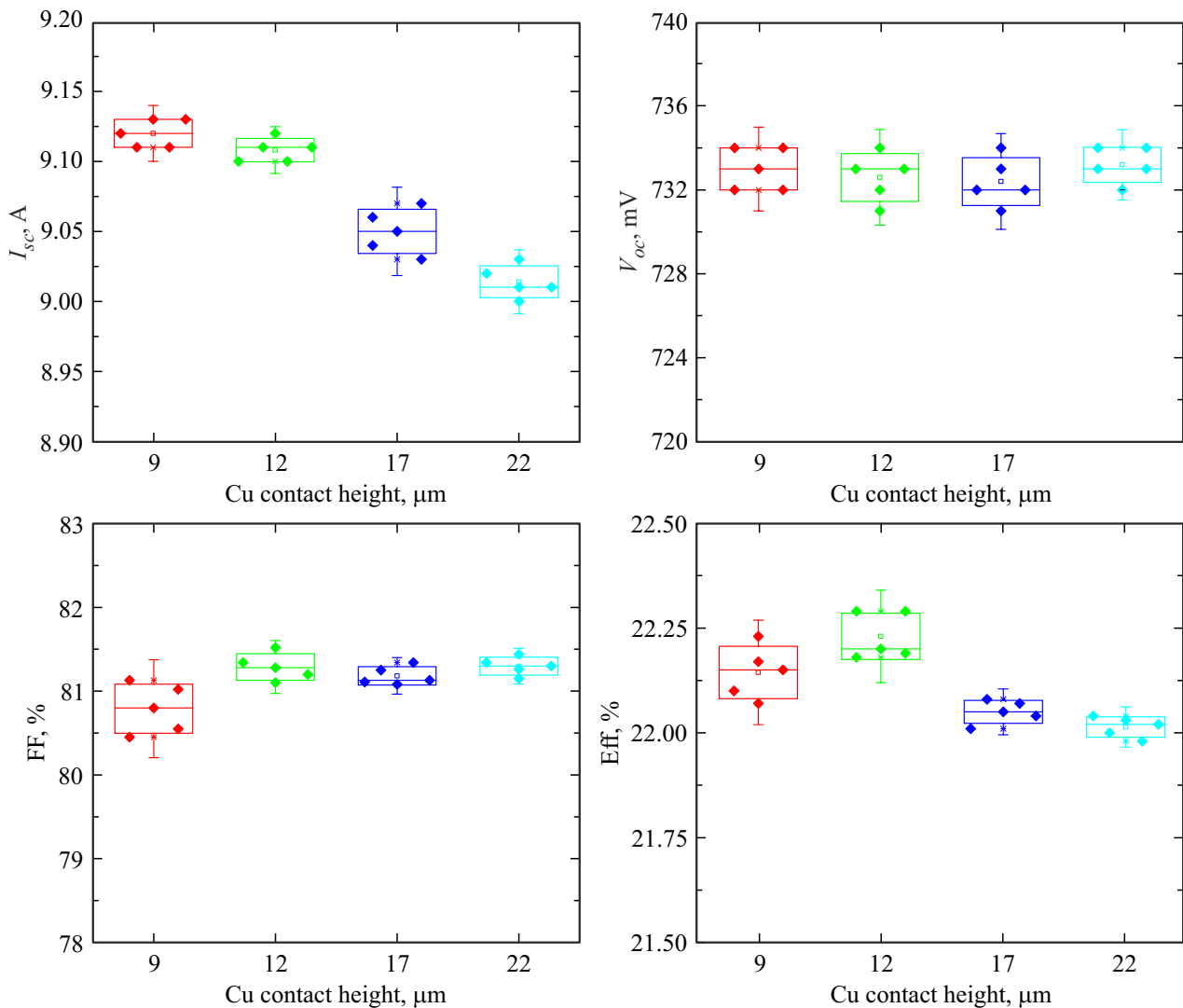
Figure 9. Parameters of SHJ PVC with copper contact grid (4BB) fabricated using the HMI mask shown in Fig. 6, depending on the height of Cu-contact paths.

Cu-contact path at its base was initially equal to $36 \pm 5 \, \mu m$ and increased as it grew up to $> 50 \, \mu m$ at the height of the contact path $h > 20 \, \mu m$. It should be noted that the height of the pyramidal relief on the surface of the SHJ PVC, which serves to reduce optical losses, was in the range from 1 to $5 \, \mu m$, while the total thickness of the ITO and metal PVD layers was 200 nm.

The results presented in Fig. 9 show that as the height of Cu-galvanic contact paths increases from 9 to $22 \, \mu m$, I_{sc} mainly decreases by 120 mA, which is consistent with the results presented in Fig. 8. Interestingly, FF reaches its maximum value at the height of $\sim 12 \, \mu m$, which is close to the optimal height for the given HMI mask geometry, and practically does not change with height. This may indicate that the series resistance in this case is limited by the contact resistance of the intermediate metal layers used to improve lateral conductivity and adhesion to the ITO layers. Depending on the conditions of their application and the type of ITO, measurements based on the TLM method showed that the contact resistance (ρ_c) for these layers lies in the range of $10-30 \, mOhm \cdot cm^2$, which agrees with the results obtained by other researchers [21]. Since acid cleaning was used before the process of electroplating the Cu-contact grid, it can be assumed that the high contact resistance is caused not by surface oxide, but by the contact of the adhesive metal layers to ITO. This fact is also confirmed by comparing the CVCs of SHJ PVCs having the same Cu- and Ag-contact grids that are busbarless (busbarless — 0BB), with approximately the same cross section of the contact paths, made by inkjet and screen printing, respectively. As can be seen from Table 3, SHJ PVC with standard Ag-grid has higher FF and lower series resistance (R_s) compared to Cu-contact grid. Whereas the cross-sectional area of their contact paths is approximately the same: $h \times w \times GF = 12 \, \mu m \times 30-35 \, \mu m \times 1$

Table 3. Comparison of SHJ PVC parameters with galvanic Cu- and screen-printed Ag-contact grids having the same geometry

Type of contact grid	Height and width of contact paths	SHJ PVC parameters				
		I_{sc}, A	V_{oc}, V	FF, %	Eff., %	R_s, Ohm $\cdot$ cm^2
Screen-printed silver contact grid (0BB)	$h = 15\,\mu m$, $w = 40-45\,\mu m$	9.25	0.740	81.47	22.61	0.0049
Grid with copper electroplated coating (0BB)	$h = 12\,\mu m$ $w = 30-35\,\mu m$	9.40	0.739	81.23	22.93	0.0045

$= 360-420\,\mu m^2$ (GF — geometric factor) and $15\,\mu m \times 40-45\,\mu m \times 0.6 = 360-402\,\mu m^2$ for Cu- and Ag-contact paths, respectively, while the specific resistance of low-temperature Ag-pastes is ~ 2 times higher than that of galvanic copper (see Table 2). Therefore, to further reduce R_s and increase the efficiency of SHJ PVC with a Cu-contact grid, further optimization of the buffer metal layers is required to reduce their contact resistance. Nevertheless, the efficiency of a SHJ PVC with a Cu-contact grid is 0.3 abs.% higher than that of a SHJ PVC with a low-temperature Ag-grid because of the decrease in optical losses due to for narrower Cu-contact paths.

Additional advantage of Cu-galvanic contacts is the possibility of their soldering when assembling SHJ modules, while most low-temperature Ag-pastes are non-solderable. In this case, the critical factor that determines the mechanical properties of the contacts is their adhesion to the ITO layers on the surface of the SHJ PVC. The results of tests using the thin ($\leq 100-200\,nm$) Cu-layer deposited on the surface of ITO layers by sputtering a Cu-target in an argon atmosphere showed its poor adhesion to the ITO surface ($< 0.5\,N/mm$) after completion of the electroplating process. In this case, the level of adhesion was determined by soldering the current-collecting busbar (width $1.0\,mm$) and its subsequent separation with an angle of $180°$ (the so-called pull force test). As the test results showed, certain combinations of Ti, Cr, NiV, and Cu PVD layers can lead to an adhesion level of $3-5\,N/mm$ approximately, which significantly exceeds the adhesion of low-temperature pastes to ITO ($1.5-2\,N/mm$) and is not insignificant when creating very narrow contact paths ($w < 30\,\mu m$).

5. Conclusion

It is shown that inkjet printing based on organic ink in combination with electroplating is a promising method for creating narrow ($< 40\,\mu m$) copper contact grids on the surface of SHJ PVC. Whereas the use of thin buffer metal layers deposited on the surface of the ITO layers by magnetron sputtering makes it possible to achieve excellent quality for adhesion of galvanic copper to ITO ($> 3\,N/mm$). Using these methods, full-size ($157 \times 157\,mm$) double-sided SHJ PVCs with Cu-contact grid with efficiency $= 22.9\%$ were fabricated. To further increase the efficiency, further optimization of the process is required, aimed at reducing

the contact resistance between the ITO and the buffer adhesive layers and optimizing the shape of the grooves in the etch-resistant organic mask with a further decrease in their width.

Conflict of interest

The authors declare that they have no conflict of interest.

References

[1] R. Preu, E. Lohmuller, S. Lohmuller, P. Saint-Cast, J.M. Greulich. Appl. Phys. Rev., **7**, 041315 (2020).

[2] A.S. Abramov, D.A. Andronikov, S.N. Abolmasov, E.I. Terukov. In: *High Efficient Low-Cost Photovoltaics, Recent Developments,* 2nd edn (Springer Nature, Switzerland, 2020) p. 113.

[3] K. Yoshikawa, H. Kawasaki, W. Yoshida, T. Irie, K. Konishi, K. Nakano, T. Uto, D. Adachi, M. Kanematsu, H. Uzu, K. Yamamoto. Nature Energy, **2**, 17032 (2017).

[4] P.J. Verlinden. J. Renewable Sustainable Energy, **12**, 053505 (2020).

[5] W. Wang. The mass production of HJT in Huasun, 4th Int. Workshop on Silicon Heterojunction Solar Cells (2021).

[6] J. Yu, J. Li, Y. Zhao, A. Lambertz, T. Chen, W. Duan, W. Liu, X. Yang, Y. Huang, K. Ding. Solar Energy Mater. & Solar Cells, **224**, 110993 (2021).

[7] S.K. Chunduri, M. Schmela. *Heterojunction solar technology* (TAIYANGNEWS Press release, 2020).

[8] D. Adachi, J.L. Hernandez, K. Yamamoto. Appl. Phys. Lett., **107**, 233506 (2015).

[9] D. Adachi, T. Terashita, T. Uto, J.L. Hernandez, K. Yamamoto. Solar Energy Mater. & Solar Cells, **163**, 204 (2017).

[10] A. Dabirian, A. Lachowicz, J.W. Schüttauf, B. Paviet-Solomon, M. Morales-Masis, A. Hessler-Wyser, M. Despeisse, C. Ballif. Solar Energy Mater. & Solar Cells, **159**, 243 (2017).

[11] A. Lachowicz, G. Andreatta, N. Blondiaux, A. Faes, N. Badel, J.J.D. Leon, C. Allébe, C. Fontaine, P.-H. Haumesser, J. Jourdan, D. Muñoz, M Godard, M. Darmon, S. Nicolay, M. Despeisse, C. Ballif. Proc. IEEE 48th Photovoltaic Specialists Conf. (2021) p. 1530.

[12] T. Hatt, J. Bartsch, S. Schellinger, J. Schneider, A.A. Brand, S. Kluska, M. Glatthaar. *Proc. 38th Eur. Photovoltaic Solar Energy Conf.* (2021) p. 326.

[13] Patent WO 2016/000030, https://www.pv-magazine.com/2021/09/10/austaralian-startup-sets-25-54-efficiency-record-for-silicon-cell

[14] J.B. Heng, J. Fu, B. Kong, Y. Chae, W. Wang, Z. Xie, A. Reddy, K. Lam, C. Beitel, C. Lioa, C. Erben, Z. Huang, Z. Xu. IEEE J. Photovoltaics, **5**, 82 (2014).

[15] DuPont^TM Riston special series data sheet & processing information

[16] D. Stüwe, D. Mager, D. Biro, J.G. Korvink. Inkjet Technology for Crystalline Silicon Photovoltaics, **27**, 599 (2015).

[17] T. Hatt, J. Bartsch, S. Kluska, S. Nold, S.W. Glunz, M. Glatthaar. *Proc. IEEE 47th Photovoltaic Specialists Conf.* (2020) p. 397.

[18] A. Lachowicz, A. Descoeudres, J. Champliaud, A. Faes, J. Geissbuhler, M. Despeisse, S. Nicolay, C. Ballif. *Proc. 36th Eur. Photovoltaic Solar Energy Conf.* (2019) p. 564.

[19] A. Lachowicz, P. Wayss, J. Geissbuhler, A. Faes, J. Champliaud, N. Badel, C. Ballif, M. Despeisse. Review on plating processes for silicon heterojunction cells, 8th Workshop on Metallization and Interconnection for Crystalline Silicon Solar Cells (2019).

[20] S. Abolmasov, A. Abramov, D. Andronikov, K. Emtsev, G. Ivanov, I. Nyapshaev, D. Orekhov, A. Semenov, G. Shelopin, E. Terukov, B. Strahm, G. Wahli, P. Papet, T. Söderström, Y. Yao, T. Hengst, G. Kekelidze. *Proc. 31th Eur. Photovoltaic Solar Energy Conf.* (2015) p. 1046.

[21] A. Aguilar, S. Herasimenka, J. Karas, H. Jain, Jongwon Lee, K. Munoz, L. Michaelson, T. Tyson, W. Dauksher, S. Bowden. *Proc. IEEE 43rd Photovoltaic Specialists Conf.* (2016) p. 972.